Theory of spin excitations in Fe(110) monolayers

R. B. Muniz* and D. L. Mills
Department of Physics and Astronomy, University of California, Irvine, California 92697
(Received 23 April 2002; published 11 November 2002)

We present theoretical studies of short-wavelength spin excitations in ferromagnetic Fe(110) monolayers either adsorbed on a W(110) substrate or free standing. We use an itinerant model of electrons as the basis for our analysis, with nine bands (the five $3d$ bands and the $4sp$ complex) included. The bands are described within an empirical tight-binding scheme, and the ferromagnetic ground state is generated from on-site intra-atomic Coulomb interactions, described in mean-field theory. The random phase approximation (RPA) is employed to describe the spin excitations through analysis of the wave vector and frequency dependence of the dynamic transverse susceptibility. Several issues are explored. We compare the spin-wave stiffness and other features of the spin-wave spectrum for the free standing film and that adsorbed on the substrate to find substantial quantitative differences with origin in spin-spin interactions mediated by the substrate. We also compare the spin-wave spectrum calculated through use of the RPA, an approximate theory, but a scheme that does not invoke the adiabatic approximation, with results generated within the framework of the adiabatic approach. While the spin-wave exchange stiffnesses produced by the two methods are in agreement, there are substantial differences between excitation spectra at short wavelengths. We argue that effective interspin exchange couplings generated within the framework of the adiabatic approximation fail to provide a description of the spin-wave spectrum in the itinerant ferromagnets, beyond the low-frequency, long-wavelength regime where the spin-wave exchange stiffness suffices to describe the spectrum. We also discuss apparent hybridization gaps in the spin-wave spectrum. We show that in some cases they can be artifact of a poorly converged numerical analysis and, in one instance, on use of an inappropriate form for the intra-atomic Coulomb interaction.

DOI: 10.1103/PhysRevB.66.174417 PACS number(s): 75.70.Ak, 75.70.Rf, 75.40.Gb

I. INTRODUCTION

The study of the magnetism in ultrathin (few atomic layer) films is pursued actively for several reasons. For example, such films are realizations of two-dimensional magnetic matter and thus provide tests of theoretical models of magnetism in less than three dimensions. The fact that a large fraction of the moment bearing ions reside in sites on the surface or interface between film and substrate leads to a strong anisotropy of the spin-orbit origin with diverse character. This endows ultrathin films and multilayers which incorporate them with unique properties not found in bulk magnetic matter. It is the case as well that exciting device applications have been realized and more are contemplated. Here multilayer structures fabricated from ultrathin ferromagnetic films provide us with nanoscale structures with unique magnetic response characteristics not realized in bulk materials.

Ultrathin ferromagnetic films formed from the $3d$ transition metals have been the principal focus of the field, since they may be grown with high quality on a number of metallic substrates. Also, their ferromagnetism persists at room temperature, a property important for applications. A very considerable effort has been devoted to the study of their electronic structure and magnetism via *ab initio* calculations.[1] Such calculations, however, focus on ground-state properties, such as the spatial distribution and nature of magnetic moments, the anisotropy, and other related matters.

Spin excitations in these systems are of fundamental interest as well, since they control their response characteristics and also enter into the description of diverse physical processes. For instance, the spin and energy dependence of hot electron mean free paths is controlled by the inelastic scattering of electrons from spin excitations[2] in the ferromagnetic transition metals. From the experimental point of view, with one exception noted below, only spin waves with wavelength very long compared to the lattice constant have been probed experimentally in ultrathin films. The two common methods to study such collective excitations are ferromagnetic resonance spectroscopy[2] and Brillouin light scattering.[3] The first excites spin waves of infinite wavelength and the second modes with wave vector in the range of 10^5 cm^{-1}. Both methods explore modes whose frequency is controlled by parameters that may be viewed as ground-state properties.[4]

It is of fundamental interest to obtain information on the dispersion relation of short-wavelength spin-wave excitations as a function of wave vector throughout the surface Brillouin zone. Such data would provide us with insight into truly microscopic aspects of the magnetic response characteristics of ultrathin films. In the case of surface phonons, electron loss spectroscopy provides a means of accessing details of their dispersion curves throughout the surface Brillouin zone for both clean and adsorbate covered surfaces.[5] These data, when analyzed, provide us with insight into details of the interatomic forces operative in the surface environment. In principle, spin-polarized electron energy loss spectroscopy (SPEELS) may be used to probe the dispersion of spin waves out to the boundary of the surface Brillouin zone. This possibility has stimulated theoretical studies in which the absolute cross section for exciting spin waves on surfaces has been calculated and compared to that for surface

phonon excitation,[6] microscopic descriptions of spin excitations in ultrathin films of Fe have been initiated,[7] and a microscopic theory of excitation of both spin waves and Stoner excitations has been developed with applications to ferromagnetic Fe.[8] Interestingly, while inelastic neutron scattering can be employed to study spin waves in the ferromagnetic metals, of course, neutrons and electrons probe very different response functions, so the spectra measured by the two methods can differ qualitatively.[9] This sequence of theoretical studies have stimulated a new SPEELS study[10] of the low-loss regime in the SPEELS spectrum of Fe, and the spin-wave signal has been detected with intensity relative to the previously observed Stoner excitations in excellent accord with theory.

It will be useful to have explicit predictions in hand regarding the nature of short-wavelength spin waves in ultrathin film/substrate combinations that will be employed in the coming generation of new experiments. While it is indeed the case that quantitative calculations have been put forward for ultrathin Fe(100) films with thickness up to seven layers,[7] these were free-standing films. The influence of the substrate on the spin excitations was thus not explored in this work. It is the case as well that the SPEELS study described in the previous paragraph employed an Fe(110) film (four layers in thickness) adsorbed on the W(110) surface. We understand future experiments will employ this system as well.[11] The Fe/W(110) system is particularly suitable for such studies, since as Gradmann has emphasized[12] in classic papers, from the thermodynamic point of view Fe wets the W surface. Thus, ultrathin films of particularly high quality can be grown for this film/substrate combination.

It is a nontrivial extension of the earlier work[7] on free-standing films to incorporate the role of the substrate on the spectrum of spin excitations in ultrathin ferromagnetic films within the framework of an itinerant electron picture and with a sufficient number of energy bands to provide a realistic description of the electronic structure of the system. In this paper, we present a detailed series of calculations of the spin-wave spectrum of a monolayer of ferromagnetic Fe on the W(110) surface. We confine our attention simply to the monolayer here, since we have found several issues that require exploration, so the set of calculations we have pursued is in fact very extensive. We shall describe multilayer films in subsequent work. We turn to a brief summary of the issues we have encountered in the course of this research.

One issue, of course, is the role of indirect spin-spin interactions through the substrate present in the adsorbed film, but absent in free-standing film. Not surprisingly, we find substantial quantitative differences in the spin-wave stiffness of the free-standing and adsorbed films. For instance, we see a large anisotropy in the exchange stiffness for the two examples. The anisotropy is substantially larger for the adsorbed film, however.

There is another issue we explore. First, we note that a number of authors generate descriptions of spin-wave excitations throughout the Brillouin zone of ultrathin films through use of an adiabatic description of spin motions.[13–16] This may be accomplished within the framework of the spin-polarized version of density functional theory. One way this may be accomplished is to rotate the spin density within a selected unit cell and then calculate the torque exerted on the moments in neighboring unit cells. One may deduce effective intersite exchange integrals from the torques so calculated. From these, through use of a description of spin waves appropriate to insulators with highly localized moments, a theoretical dispersion curve is constructed.

Our calculations do not resort to such an adiabatic approximation, but are based on application of the random phase approximation (RPA) to a description of the spin response of our itinerant ferromagnet. Thus, as in previous treatments of the spin dynamics of such systems[7,17] we include the Landau damping overlooked in approaches built around the adiabatic approximation. As pointed out many years ago by Cooke and collaborators,[17] Landau damping can be severe at short wavelengths. In ultrathin films, because wave vectors perpendicular to the surface need not be conserved in the Landau damping events, we can expect its role to be more dramatic than in bulk ferromagnets. The calculations reported below show that short-wavelength spin waves are indeed strongly damped for the adsorbed film. Indeed, the earlier studies of free-standing ultrathin Fe(100) films within the framework used here showed that the damping can become so severe that high-lying standing-spin-wave resonances are washed out in the relevant spectral densities. It is thus clear that the adiabatic approach would yield qualitatively incorrect conclusions regarding the spin-wave spectrum of ultrathin itinerant electron films, since all standing-wave modes would be described as infinitely long lived in this picture.

In the present paper, we report explicit comparisons between calculations based on the full dynamical theory and calculations carried out by means of the adiabatic approach each applied to the same system. As argued some years ago[18] we find that indeed both approaches provide us with precisely the same value for the exchange stiffness that controls the dispersion of very-long-wavelength, low-frequency spin waves. But we see substantial differences for the dispersion relation provided by the two approaches as we move out into the surface Brillouin zone. The differences are qualitative, not a matter of quantitative detail. It is clear from simple reasoning that allowing the electrons to respond dynamically to spin motions not only introduces Landau damping, but also has a strong effect on the dispersion curve itself. One may argue that by incorporating the dynamical response of the electron system in the description of the spin wave, in essence, one renormalizes the collective excitation by providing it with a self-energy. The imaginary part of the self-energy gives rise to a finite width in the spin-wave spectral density, i.e., the Landau damping. Simple considerations along the lines which lead to the Kramers-Kronig relation assure one that there must be a reactive or real part to the self-energy, which renormalizes the dispersion curve. When the Landau damping is strong, as it is in these systems, the real part of the self-energy is appreciable as well. The RPA used here does not, of course, provide us with a rigorous description of the spin-wave dispersion at short wavelengths, but we argue it does incorporate essential physics omitted from the adiabatic descriptions.

The outline of this paper is as follows. In Sec. II, we describe the formalism we have used to perform the calculation of the dynamic transverse susceptibility of the ultrathin film, when it is adsorbed on the W(110) substrate. Then Sec. III presents the results for the adsorbed and free-standing monolayers and discusses their relation to dispersion curves calculated with use of the adiabatic approach. We also here address the question of apparent hybridization gaps which can appear in calculated spectra. We demonstrate that in some cases these can be artifacts which disappear in fully converged calculations when ones utilizes intra-atomic Coulomb interactions of appropriate structure.

We remark that the virtue of the scheme employed in this paper is that it allows studies of spin excitations of a film adsorbed on a substrate treated as fully semi-infinite in nature; within full time-dependent density-functional-based studies, such geometries remain a challenge to address.

We conclude this section with comments on the influence of dipolar interactions, neglected here, on the results we present below. Quite generally, in ferromagnets, the energy scale associated with dipolar interaction strengths (≈ 1 K or 0.1 meV) is orders of magnitude smaller than that associated with effective exchange interactions within the spin system (≈ 100 meV in the materials of interest here). However, when very-long-wavelength, low-frequency spin waves are excited in ferromagnetic resonance or Brillouin light scattering experiments, exchange contributions are modest or perhaps even neglibile often, since the angle between nearby excited spins is very small and the range of effective exchange interactions is microscopic. In such circumstances, the dipolar interactions assert themselves most importantly. Of interest to us, as noted about, are modes of rather short wavelength, where exchange effects strongly dominate the dipolar contributions to the excitation energy. We direct the reader to an earlier study,[19] where the transition from the long-wavelength dipolar-dominated regime to the short-wavelength exchange-dominated regime is studied in detail for ultrathin ferromagnetic films. The crossover is at wavelengths far longer than can be probed in a SPEELS experiment, as one can see from this discussion.

II. TRANSVERSE SPIN SUSCEPTIBILITY

The formalism we have used to calculate the dynamic transverse susceptibility of the ultrathin film follows that of Ref. 7. An atomic orbital basis is introduced, and the electronic structure of the system is described by a general multiorbital tight-binding model Hamiltonian

$$H=\sum_{ij}\sum_{\mu\nu\sigma} T_{ij}^{\mu\nu} c_{i\mu\sigma}^{\dagger} c_{j\nu\sigma} + H_{int}, \tag{1}$$

where $c_{i\mu\sigma}^{\dagger}$ creates an electron of spin σ in atomic orbital μ on the site at $\vec{R}_i$. The first term of H represents the electronic kinetic energy plus a spin-independent local potential, and H_{int} is the electron-electron interaction term. The transfer integrals $T_{ij}^{\mu\nu}$ are parametrized following the standard Slater-Koster (SK) tight-binding (TB) formalism.[20] We shall assume that the effective electron-electron interaction U is of short range and keep only on-site interactions in H_{int}. In this case,

$$H_{int}=\frac{1}{2}\sum_{\mu\nu}\sum_{\mu'\nu'}\sum_{i\sigma\sigma'} U_{i;\mu\nu,\mu'\nu'} c_{i\mu\sigma}^{\dagger} c_{i\nu\sigma'}^{\dagger} c_{i\nu'\sigma'} c_{i\mu'\sigma}, \tag{2}$$

where $U_{i;\mu\nu,\mu'\nu'}$ is a matrix element of the effective electron interaction between orbitals, all centered on the same site i. The substrate will be assumed to contain noninteracting electrons, so the intra-atomic Coulomb interactions are nonzero only within the ferromagnetic film.

In order to take advantage of translational symmetry parallel to the layers, it is convenient to work with a mixed representation by choosing our basis as Bloch sums in a single atomic plane l:

$$|l,\vec{q}_{\parallel};\mu\sigma\rangle=\frac{1}{N_{\parallel}}\sum_{i\in l}|i;\mu\sigma\rangle e^{i\vec{q}_{\parallel}\cdot\vec{R}_i}. \tag{3}$$

Here $N_{\parallel}$ is the number of sites in plane l and $\vec{q}_{\parallel}$ is a wave vector parallel to the layers.

The dynamic transverse spin susceptibility $\chi^{+-}(ll';\vec{q}_{\parallel},\omega)$ is defined in terms of the time Fourier transform of the two-particle retarded Green function

$$G^{+-}(ll';\vec{q}_{\parallel},t)=-i\Theta(t)\langle[S_{\vec{q}_{\parallel}}^{+}(l,t),S_{-\vec{q}_{\parallel}}^{-}(l',0)]\rangle. \tag{4}$$

The operators $S_{\vec{q}_{\parallel}}^{\pm}(l,t)$ are two-dimensional Fourier transforms of the corresponding spin raising and lowering operators $S_i^{\pm}(t)$ on the film lattice sites $i\in l$. Explicit representations of these operators are given elsewhere.[7] The brackets denote a commutator, $\langle\cdots\rangle$ the thermodynamical average, which reduces to the ground-state expectation value at zero temperature, and $\Theta(t)$ is the usual step function, equal to unity for $t>0$ and zero otherwise.

By solving the equation of motion for $G^{+-}(ll';\vec{q}_{\parallel},t)$ within the RPA and assuming $U\neq 0$ only at the lattice sites of the ferromagnetic ultrathin film, one finds

$$\chi^{+-}(ll';\vec{q}_{\parallel},\omega)=\sum_{\mu\nu}\sum_{\mu'\nu'} F_{\mu\nu}(\vec{q}_{\parallel}) \times G_{\mu\nu,\mu'\nu'}(ll';\vec{q}_{\parallel},\omega)F_{\mu'\nu'}(-\vec{q}_{\parallel}), \tag{5}$$

where $F_{\mu\nu}(\vec{q}_{\parallel})=\langle i\mu|e^{-i\vec{q}_{\parallel}\cdot\vec{r}}|i\nu\rangle$ is a magnetic form factor and $G_{\mu\nu,\mu'\nu'}(ll';\vec{q}_{\parallel},\omega)$ satisfies the equation

$$G_{\mu\nu,\mu'\nu'}(ll';\vec{q}_{\parallel},\omega)=G^{0}_{\mu\nu,\mu'\nu'}(ll';\vec{q}_{\parallel},\omega) -\sum_{\gamma\delta}\sum_{\alpha\beta}\sum_{l''} G^{0}_{\mu\nu,\gamma\delta}(ll'';\vec{q}_{\parallel},\omega) \times U_{\gamma\beta,\alpha\delta}G_{\beta\alpha,\mu'\nu'}(l''l';\vec{q}_{\parallel},\omega). \tag{6}$$

The function $G^0_{\mu\nu,\mu'\nu'}(ll';\vec{q}_\parallel,\omega)$, defined by Eq. (2.23) of Ref. 7 for films of arbitrary but finite thickness, can be used to construct the noninteracting susceptibility $\chi^0(ll';\vec{q}_\parallel,\omega)$ by using a prescription analogous to that in Eq. (5). Here, however, since we are dealing with a film adsorbed on a semi-infinite substrate, it is necessary for our numerical work to express G^0 in terms of one-electron propagators as follows:

$$G^0_{\mu\nu,\mu'\nu'}(ll';\vec{q}_\parallel,\omega)=\frac{1}{N_\parallel}\sum_{\vec{k}_\parallel}\int d\omega' f(\omega')$$
$$\times[\mathcal{I}\mathrm{m}\, g^{\uparrow}_{l'\nu'l\mu}(\vec{k}_\parallel,\omega')g^{\downarrow}_{l\nu l'\mu'}(\vec{q}_\parallel+\vec{k}_\parallel,\omega'+\omega)$$
$$+\mathcal{I}\mathrm{m}\, g^{\downarrow}_{l\nu l'\mu'}(\vec{q}_\parallel+\vec{k}_\parallel,\omega')g^{-\uparrow}_{l'\nu'l\mu}(\vec{k}_\parallel,\omega'-\omega)], \tag{7}$$

where $f(\omega)$ is the usual Fermi distribution function, g and g^- represent the retarded and advanced one-particle Green functions, respectively, and

$$\mathcal{I}\mathrm{m}\, g=\frac{i}{2\pi}[g-g^-]. \tag{8}$$

Equation (6) can be solved, and in matrix notation it takes the rather general form

$$G(\vec{q}_\parallel,\omega)=[1+G^0(\vec{q}_\parallel,\omega)U]^{-1}G^0(\vec{q}_\parallel,\omega), \tag{9}$$

where 1 represents the unit matrix.

Numerical calculations of $\chi^{+-}(ll';\vec{q}_\parallel,\omega)$ require G^0 to be determined as accurately and reliably as possible. It is noteworthy that both g and g^- are not very smooth functions of ω', particularly when the imaginary part usually added to their energy argument (in order to displace their singularities from the real axis) becomes very small. For this reason, we find that evaluating the ω' integral over the real axis in Eq. (7) directly is not the most efficient and accurate way of calculating G^0. We notice, however, that by substituting Eq. (8) into Eq. (7), we may write $G^0=I_1+I_2+I_3$, where

$$I_1=\frac{i}{2\pi N_\parallel}\sum_{\vec{k}_\parallel}\int d\omega' f(\omega')$$
$$\times[g^{\uparrow}_{l'\nu'l\mu}(\vec{k}_\parallel,\omega')g^{\downarrow}_{l\nu l'\mu'}(\vec{q}_\parallel+\vec{k}_\parallel,\omega'+\omega)], \tag{10}$$

$$I_2=-\frac{i}{2\pi N_\parallel}\sum_{\vec{k}_\parallel}\int d\omega' f(\omega')$$
$$\times[g^{-\downarrow}_{l\nu l'\mu'}(\vec{q}_\parallel+\vec{k}_\parallel,\omega')g^{-\uparrow}_{l'\nu'l\mu}(\vec{k}_\parallel,\omega'-\omega)], \tag{11}$$

and

$$I_3=\frac{i}{2\pi N_\parallel}\sum_{\vec{k}_\parallel}\int d\omega'[f(\omega'+\omega)-f(\omega')]$$
$$\times g^{\downarrow}_{l\nu l'\mu'}(\vec{q}_\parallel+\vec{k}_\parallel,\omega'+\omega)g^{-\uparrow}_{l'\nu'l\mu}(\vec{k}_\parallel,\omega'). \tag{12}$$

I_1 and I_2 are most easily evaluated as contour integrals in the complex-ω' plane. At finite temperatures T, the integration over ω' can be replaced by a sum over imaginary Matsubara frequencies $\omega'_n=(2n+1)\pi k_B T$. This is achieved by closing the contour with an infinite-radius semicircle going counter clockwise in the upper-half complex plane for I_1, and clockwise in the lower-half plane for I_2. At $T=0$, we end up with

$$I_1+I_2=\frac{1}{2\pi N_\parallel}\sum_{\vec{k}_\parallel}\int_{0^+}^{\infty}d\eta[g^{\uparrow}_{l'\nu'l\mu}(\vec{k}_\parallel,E_F+i\eta)$$
$$\times g^{\downarrow}_{l\nu l'\mu'}(\vec{q}_\parallel+\vec{k}_\parallel,E_F+\omega+i\eta)$$
$$+g^{\uparrow *}_{l\mu l'\nu'}(\vec{k}_\parallel,E_F-\omega+i\eta)$$
$$\times g^{\downarrow *}_{l'\mu' l\nu}(\vec{q}_\parallel+\vec{k}_\parallel,E_F+i\eta)], \tag{13}$$

where E_F is the Fermi energy and we have made use of the fact that $g^-_{l\nu l'\mu'}(\vec{k}_\parallel,z)=g^*_{l'\mu' l\nu}(\vec{k}_\parallel,z^*)$.

This method of evaluating I_1+I_2 is numerically more efficient for various reasons: it assures that all states beneath E_F are properly taken into account, the integrand as a function of η is much smoother, and the numerical generation of the one-electron Green functions as well as the summation over $\vec{k}_\parallel$ usually converges faster for increasing values of η. Unfortunately the same simple procedure does not apply to I_3 because it involves the product gg^-, and g is an analytic function of ω' in the upper-half complex plane, whereas g^- is analytic in the lower-half plane. Nevertheless, owing to the Fermi functions in Eq. (12), at $T=0$ I_3 reduces to

$$I_3=-\frac{i}{2\pi N_\parallel}\sum_{\vec{k}_\parallel}\int_{E_F-\omega}^{E_F}d\omega' g^{\downarrow}_{l\nu l'\mu'}(\vec{q}_\parallel+\vec{k}_\parallel,\omega'+\omega)$$
$$\times g^{\uparrow *}_{l\mu l'\nu'}(\vec{k}_\parallel,\omega'). \tag{14}$$

It should be stressed that I_3 does not contribute to static properties of the system, including, for example, the spin-wave stiffness constant D which we shall see is proportional to $\lim_{\vec{q}_\parallel\to 0}q_\parallel^2\chi^{+-}(\vec{q}_\parallel,0)$, because $I_3=0$ for $\omega=0$.

The first step in the calculation of $\chi^{+-}(\vec{q}_\parallel,\omega)$ is to obtain the one-electron Green functions $g^{\sigma}_{l\mu l'\nu}(\vec{q}_\parallel,\omega)$ which are used to construct G^0. In order to simplify the notation we treat $g^{\sigma}_{ll'}(\vec{k}_\parallel,\omega)$ as a matrix in orbital indices with elements $g^{\sigma}_{l\mu l'\nu}(\vec{q}_\parallel,\omega)$. Here we are interested in a monolayer of Fe adsorbed on a W(110) semi-infinite substrate. We label the surface Fe atomic plane by $l=1$ and shall calculate $\chi^{+-}(\vec{q}_\parallel,\omega)\equiv\chi^{+-}(11;\vec{q}_\parallel,\omega)$, which involves only g functions associated with $l=l'=1$. The calculation of the one-electron Green function $g^{\sigma}_{11}(\vec{k}_\parallel,\omega)$ within the Fe overlayer is performed as follows: we start with the surface Green function of the isolated semi-infinite substrate $g^0_{00}(\vec{k}_\parallel,\omega)$, which

is obtained by well-established numerical methods.[21] The atomic monolayer of Fe is then adsorbed on this surface by switching on the hopping matrices $h_{01}(\vec{k}_\parallel)$ and $h_{10}(\vec{k}_\parallel)$ between the substrate and the monolayer. Using Dyson's equation we find

$$g_{11}^{\sigma}(\vec{k}_\parallel,\omega)=[\omega-h_{11}^{\sigma}(\vec{k}_\parallel)-h_{10}(\vec{k}_\parallel)g_{00}^{0}(\vec{k}_\parallel,\omega)h_{01}(\vec{k}_\parallel)]^{-1}, \tag{15}$$

where $h_{11}^{\sigma}(\vec{k}_\parallel)$ represents the one-electron Hamiltonian matrix of the isolated Fe monolayer.

As long as H_{int} is an on-site interaction, the matrix elements of $h_{11}^{\sigma}(\vec{k}_\parallel)$ take the form

$$h_{\mu\nu}^{\sigma}(\vec{k}_\parallel)=T_{\mu\nu}(\vec{k}_\parallel)-\frac{1}{2}\Delta_\mu\delta_{\mu\nu}\sigma, \tag{16}$$

where $\sigma=\pm1$ for $\uparrow$ and $\downarrow$ spin, respectively. Here Δ_μ symbolize the exchange splitting associated with orbital μ, generally given by[7]

$$\Delta_\mu=\sum_\nu J_{\mu\nu}m_\nu, \tag{17}$$

where $m_\nu=n_{\nu\uparrow}-n_{\nu\downarrow}$ is the contribution from orbital ν to the overlayer magnetic moment $m=\Sigma_\nu m_\nu$, $n_{\nu\sigma}$ is number of electrons with spin σ in this orbital, and the exchange integrals $J_{\mu\nu}=U_{\mu\nu,\nu\mu}$. There are, of course, contributions to the electron self-energy proportional to $n_\nu=n_{\nu\uparrow}+n_{\nu\downarrow}$. Within our scheme, these are independent of $\vec{k}_\parallel$ and are absorbed in $T_{\mu\nu}(\vec{k}_\parallel)$. It should be noted as well that when the quantities $T_{ij}^{\mu\nu}$ in Eq. (1) are extracted from empirical fits to *ab initio* electronic structure calculations of the paramagnetic state, they contain Coulomb contributions. A procedure for correcting for this within our scheme is described in Ref. 7. In order to further simplify the notation hereinafter we omit the plane indices $l=l'=1$.

Owing to the relatively small spin polarization of the *sp* states and the much more localized nature of the *d* orbitals, it is reasonable to consider the effective Coulomb interaction in transition-metal ferromagnets as taking place only within the *d* orbitals. In this case, all the matrix elements of *U* involving *s* or *p* orbitals may be approximately set equal to zero, and as a first approximation, we may take $\Delta_\mu=0$ when μ is not a *d* orbital.

Before we calculate $\chi^{+-}(\vec{q}_\parallel,\omega)$ for large values of $q_\parallel$, it is instructive to investigate the long wavelength regime analytically. In the limit of small $\vec{q}_\parallel$ the spin-wave energies vary quadratically with $q_\parallel$ ($\hbar\omega=Dq_\parallel^2$), and they appear as poles of $\chi^{+-}(\vec{q}_\parallel,\omega)$. That this is so is rigorously correct; when $q_\parallel$ is so small, all but the quadratic term in the dispersion relation may be ignored. Landau damping is of order $q_\parallel^4$ at sufficiently long wavelengths, so in the limit considered the spin wave pole lies in the real axis. According to Eq. (9), this means the matrix $[1+G^0(\vec{q}_\parallel,Dq_\parallel^2)U]$ is singular or, equivalently, that the matrix equation

$$[1+G^0(\vec{q}_\parallel,Dq_\parallel^2)U]y(\vec{q}_\parallel)=0 \tag{18}$$

has a nontrivial solution for low values of $q_\parallel$. Actually, owing to the spin rotation invariance of our Hamiltonian and the Goldstone theorem, we know that $\chi^{+-}(\vec{q}_\parallel,\omega)$ must have a pole at $\vec{q}_\parallel=0$ and $\omega=0$ associated with the Goldstone mode. In other words,

$$y_{\mu\nu}^{(0)}+\sum_{\alpha\beta}\sum_{\eta\xi}G_{\mu\nu,\alpha\beta}^{0}(0,0)U_{\alpha\beta,\eta\xi}y_{\eta\xi}^{(0)}=0 \tag{19}$$

must have a nontrivial solution $y^{(0)}\equiv y(0)$. This mode corresponds to a rigid rotation of all the magnetic moments in the system. In fact, we may show that the vector $y^{(0)}$ with components $y_{\mu\nu}^{(0)}=m_\mu\delta_{\mu\nu}$ satisfies Eq. (19). In order to verify this, we first notice that for this choice

$$\sum_{\eta\xi}U_{\alpha\beta,\eta\xi}y_{\eta\xi}^{(0)}=\sum_{\eta}U_{\alpha\beta,\eta\eta}m_\eta=\Delta_{\alpha\beta}, \tag{20}$$

where $\Delta_{\alpha\beta}$ are the matrix elements of the exchange splitting in the mean-field or Hartree-Fock (HF) approximation. Because of symmetry, only the diagonal elements of $\Delta_{\alpha\beta}$ are nonzero, i.e., $\Delta_{\alpha\beta}=\Delta_\alpha\delta_{\alpha\beta}$, as explicitly shown in Refs. 7 and 22. Thus, Eq. (19) reduces to

$$m_\mu\delta_{\mu\nu}+\sum_\alpha G_{\mu\nu,\alpha\alpha}^{0}(0,0)\Delta_\alpha=0. \tag{21}$$

With the aid of Eqs. (7), and (8) we may write

$$\begin{aligned}G_{\mu\nu,\alpha\alpha}^{0}(0,0)\Delta_\alpha=\frac{i}{2\pi N_\parallel}\sum_{\vec{k}_\parallel}\int d\omega' f(\omega')\\ \times[g_{\nu\alpha}^{\downarrow}(\vec{k}_\parallel,\omega')\Delta_\alpha g_{\alpha\mu}^{\uparrow}(\vec{k}_\parallel,\omega')\\ -(g_{\mu\alpha}^{\uparrow}(\vec{k}_\parallel,\omega')\Delta_\alpha g_{\alpha\nu}^{\downarrow}(\vec{k}_\parallel,\omega'))^*].\end{aligned} \tag{22}$$

Since the one-electron propagators for up and down spins are related by the Dyson equation

$$g_{\mu\nu}^{\uparrow}-g_{\mu\nu}^{\downarrow}=-\sum_\alpha g_{\mu\alpha}^{\downarrow}\Delta_\alpha g_{\alpha\nu}^{\uparrow}, \tag{23}$$

the second term of Eq. (21) may be rewritten as

$$\begin{aligned}\sum_\alpha G_{\mu\nu,\alpha\alpha}^{0}(0,0)\Delta_\alpha=\frac{1}{\pi N_\parallel}\sum_{\vec{k}_\parallel}\int d\omega' f(\omega')\\ \times[\mathcal{I}\mathrm{m}\, g_{\nu\mu}^{\downarrow}(\vec{k}_\parallel,\omega')\\ -\mathcal{I}\mathrm{m}\, g_{\nu\mu}^{\uparrow}(\vec{k}_\parallel,\omega')].\end{aligned} \tag{24}$$

With the help of the great orthogonality theorem of group theory[23] one can show that the summation over $\vec{k}_\parallel$ in Eq. (24) vanishes for $\mu\neq\nu$, and when $\mu=\nu$ it immediately reduces to

$$\sum_\alpha G_{\mu\mu,\alpha\alpha}^{0}(0,0)\Delta_\alpha=-m_\mu, \tag{25}$$

which completes the proof.

By expanding $y(\vec{q}_\parallel)$ and $G^0(\vec{q}_\parallel, Dq_\parallel^2)$ in Eq. (18) in powers of $q_\parallel$ for a given direction of $\vec{q}_\parallel$ and following basically the same steps of Sec. 3.2 of Ref. 18, conveniently adapted to the slab geometry, it is also possible to show that the long-wavelength spin-wave energy, correct to order $q_\parallel^2$, is given by

$$\hbar\omega_{\vec{q}_\parallel} = \frac{1}{m}\left(\sum_{\mu\nu}\Delta_\mu G^0_{\mu\mu,\nu\nu}(\vec{q}_\parallel,0)\Delta_\nu + \sum_\mu \Delta_\mu m_\mu\right), \quad (26)$$

where the magnetic moment $m=\Sigma_\mu m_\mu$.

As expected, in this limit $\hbar\omega_{\vec{q}_\parallel}$ involves only the static noninteracting response function $G^0(\vec{q}_\parallel,0)$, because D is a ground-state property of the ferromagnet. The expression in Eq. (26) is valid for a rather general form of the effective Coulomb interaction. A major requirement, of course, is that it must preserve spin rotational invariance in order to satisfy the Goldstone theorem. It is noteworthy that the spin-wave dispersion for small $\vec{q}_\parallel$ does not involve the explicit form of the U matrix, but only the exchange splittings Δ_μ and the one-electron Green functions associated with the mean-field ground state. The latter, however, is unambiguously determined by the set of Δ_μ, which in turn relies on the exchange integrals only. As long as the spin-polarized one-electron properties of the ferromagnet are well parametrized by a suitable set of Δ_μ, Eq. (26) provides a convenient way of calculating the long-wavelength spin-wave energies, regardless of the precise form of Coulomb interaction leading to those values of Δ_μ. There is thus a certain degree of freedom for choosing different sets of $U_{\mu\nu,\mu'\nu'}$ leading to the same mean-field ground state, hence to the same value of D. However, as we move away from $\vec{q}_\parallel \approx 0$, and use a proper dynamic theory to study the spin excitations (the RPA in our case) the results will be sensitive to the details of the U matrix.

With the aid of Eqs. (10) and (11), we may rewrite Eq. (26) as

$$\hbar\omega_{\vec{q}_\parallel} = \frac{4}{m}[J(0) - J(\vec{q}_\parallel)], \quad (27)$$

where

$$J(\vec{q}_\parallel) = \frac{1}{4\pi N_\parallel}\mathrm{Im}\sum_{\vec{k}_\parallel}\int d\omega' f(\omega')\sum_{\mu\nu}\Delta_\mu \times g^\downarrow_{\mu\nu}(\vec{k}_\parallel + \vec{q}_\parallel, \omega')\Delta_\nu g^\uparrow_{\nu\mu}(\vec{k}_\parallel, \omega') \quad (28)$$

is the in-plane Fourier transform of the effective exchange interaction between the Fe local magnetic moments, given by

$$J_{ij} = \frac{1}{4\pi}\mathrm{Im}\int d\omega' f(\omega')\sum_{\mu,\nu}\Delta_\mu g^\uparrow_{i\mu,j\nu}(\omega)\Delta_\nu g^\downarrow_{j\nu,i\mu}(\omega), \quad (29)$$

where i,j label atomic sites in surface plane $l=1$.

A similar set of equations [from Eqs. (26)–(29)] may be derived, alternatively, within an adiabatic description of the spin motions.[13,15,14] An equivalent expression for J_{ij} may be obtained with the use of the so-called "local force theorem"[15,24,14,25] and the spin-wave energies calculated by Eqs. (27) and (28). Our analysis explicitly shows that spin-wave energies generated by the adiabatic approach in this way are correct only in the long-wavelength limit, i.e., to order $q_\parallel^2$, and give only the spin-wave stiffness constant D correctly, as demonstrated many years ago.[18] Recent authors have also noted this point.[15] Therefore, one should not ascribe major significance to structures in the spin-wave dispersion relation obtained by such an approach when applied to wave vectors sufficiently large that the quadratic variation of frequency with wave vector no longer holds.

III. APPLICATION TO Fe(110) MONOLAYERS

In our description of the electronic structure we have employed empirical SK TB parameters for the $3d$, $4s$, and $4p$ orbitals, taking into account hopping integrals to second nearest neighbors in the two-center approximation. We start with a paramagnetic system and include the Coulomb interaction in the mean-field approximation to generate the spin-polarized one-electron ground state self-consistently. The TB parameters for all the bcc W(110) atomic planes were obtained from a first-principles linear muffin-tin orbital (LMTO) TB electronic structure calculation of bulk W,[26] and those for paramagnetic Fe were taken from Ref. 27. First-principles calculations for an Fe monolayer adsorbed on W(110) found the Fe-W interlayer spacing is relaxed downwards in comparison with the average of the bulk Fe-Fe and W-W (110) interplane distances by approximately 9.5%.[28] Since this is much closer to the Fe-Fe 110 interplanar distance, we have assumed the Fe-W hopping in our calculations equal to the Fe-Fe hopping. We consider a common Fermi energy for the substrate and overlayer and adjust the center of the d bands in the Fe atomic plane by imposing local charge neutrality at the surface. For simplicity, we have assumed a single exchange splitting $\Delta_\mu = Im$ common to all d orbitals, where I is the Stoner interaction. This seems a fair approximation for transition metal ferromagnets, at least on average for energies around E_F.[29] The observed ratio of exchange splitting to moment is $I \approx 1$ eV/μ_B for ferromagnetic $3d$ metals, and this relation approximately holds also for other low-dimensional structures, including Fe thin films.[30] We have thus performed the magnetic self-consistency assuming a fixed value of $I=1$ eV/μ_B. The resulting magnetic moment of the Fe overlayer is $m=2.17\mu_B$, which is in very good agreement with previous first-principles calculations for Fe/W(110).[28] The LDOS for majority and minority spins on the Fe surface (110) plane and subsurface W atomic plane are shown in Fig. 1. They also agree very well with results of *ab initio* calculations.[28] As expected, a very small spin polarization is induced by the Fe surface layer on the tungsten substrate, and we found the interface W atomic plane is negatively polarized with respect to the Fe film magnetization, with a magnetic moment $m=-0.05\mu_B$. The one-electron Green functions $g^\sigma_{\mu\nu}(\vec{q}_\parallel,\omega)$ associated with this ferromagnetic ground state are then used to construct G^0 according to Eqs. (13), and (14).

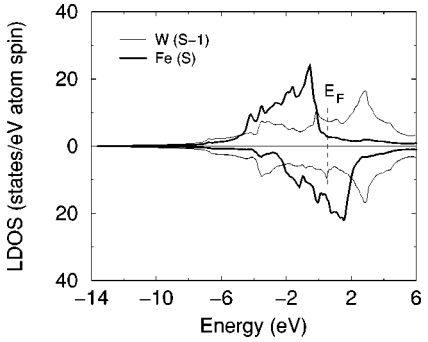

FIG. 1. Local density of states for majority and minority spins calculated for an Fe monolayer adsorbed on W(110) (thick line) and for the W atomic plane at the interface with the Fe film (thin line). The upper and lower parts of the figure correspond to majority- and minority-spin states, respectively. The vertical dashed line marks the position of the Fermi energy.

A. Long-wavelength spin waves

We begin by calculating the long-wavelength spin-wave energies in Fe/W(110) for different $\vec{q}_\parallel$ using the static approach of Eq. (26). Our results for $\vec{q}_\parallel$ along the Γ-X and Γ-L directions of the two-dimensional (2D) Brillouin zone are displayed in Fig. 2. They show that the spin-wave energies follow a quadratic dispersion relation $\hbar\omega = Dq_\parallel^2$ for low values of $q_\parallel$. However, owing to the spatial anisotropy of the (110) two-dimensional lattice, the stiffness constant D depends upon the direction $\hat{q}_\parallel$ along which the spin wave is excited. We have found $D_{\Gamma X} = 400$ meV Å^2 and $D_{\Gamma L} = 107$ meV Å^2, revealing a very large difference indeed between D along Γ-X and Γ-L in the monolayer of Fe adsorbed on W(110). It is also worth noticing that those values of D are rather different from the spin wave stiffness constant of bulk Fe, which is ≈ 300 meV Å^2 at low temperatures.

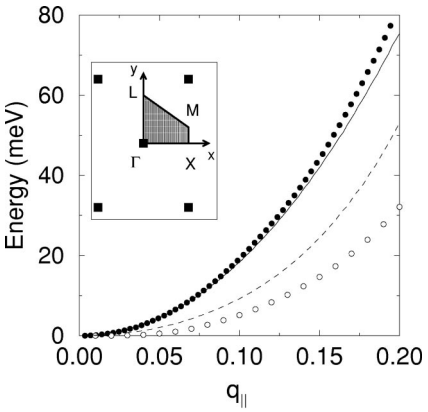

FIG. 2. Long-wavelength spin-wave energies calculated as functions of the wave vector $\vec{q}_\parallel$ along two different directions in the two-dimensional Brillouin zone for the Fe(110) monolayer. The solid and open circles represent results for the adsorbed Fe film on W(110) calculated for $\vec{q}_\parallel$ along the Γ-X and Γ-L directions, respectively. The inset shows a schematic representation of the irreducible two-dimensional Brillouin zone and some of its high-symmetry points; the solid squares symbolize reciprocal lattice points. The solid and dashed lines represent results for a free-standing Fe(110) monolayer calculated for $\vec{q}_\parallel$ along the Γ-X and Γ-L directions, respectively.

The energy necessary to excite spin waves in a ferromagnetic ultrathin film is certainly affected by the exchange interaction mediated by the nonmagnetic metallic substrate. The substrate may also significantly alter the Landau damping, modifying the spin-wave lifetimes.[31] In order to investigate the influence of the tungsten substrate on the long-wavelength spin-wave energy spectra of the Fe monolayer, we have also calculated the spin-wave energies for a free-standing Fe(110) atomic plane. Here it is more convenient to work entirely in momentum space, expressing $G^0_{\mu\mu,\nu\nu}(\vec{q}_\parallel,0)$ in terms of the eigenvalues and eigenvectors of the one-electron Hamiltonian, as originally defined by Eq. (2.23) of Ref. 7, and evaluate the two-dimensional Brillouin zone integrations by the linear triangular method (this is a straightforward 2D adaptation of the well-established linear analytic tetrahedron method[32]). We could have used a completely new set of TB parameters to describe the unsupported monolayer, obtaining them, for example, by properly fitting a first-principles band-structure calculation. However, in order to make the comparison with our previous results for Fe/W(110) more meaningful, we kept the same Fe hopping parameters, but re-evaluate the atomic-orbital energy levels in the free-standing Fe monolayer as follows: first we calculate the local orbital-occupation numbers of the surface of a semi-infinite paramagnetic Fe system, using the bulk Fe TB parameters, shifting, however, the d-band center in the surface plane to make it electrically neutral (locally). The atomic energy levels ϵ^0_μ in the unsupported monolayer were then obtained by requiring its orbital-occupation numbers to be equal to those of the Fe(110) surface. After finding the values of ϵ^0_μ for the paramagnetic state, we perform the magnetic self-consistency as described earlier, i.e., by splitting the up- and down-spin d levels in the monolayer by $\Delta = Im$, with $I = 1$ eV/μ_B. Considering the *ad hoc* approximations and hypothesis we have made, the resulting magnetic moment $m = 2.6\mu_B$ obtained by such procedure agrees fairly with the value $2.9\mu_B$ found by first-principles calculations.[33] In Fig. 3 we compare the local density of states (LDOS) for the free-standing and adsorbed Fe films. One clearly sees that hybridization effects with the wider nonmagnetic bands of the tungsten substrate considerably smoothen the LDOS of the Fe overlayer and make it acquire a rather long tail. In Fig. 2 we compare the long-wavelength spin-wave energies calculated for the free-standing and adsorbed Fe (110) monolayers for wave vectors $\vec{q}_\parallel$ along the ΓX and ΓL directions. We notice that the tungsten substrate has very little influence on the long-wavelength spin-wave excitations along ΓX, but strongly affects those in the ΓL direction by softening the spin-wave exchange stiffness considerably. The calculated values of the spin-wave stiffness constants for the Fe(110) free-standing monolayer are $D_{\Gamma X} = 382$ meV Å^2 and $D_{\Gamma L} = 192$ meV Å^2, respectively. Earlier calculations[34] for an Fe(100) unsupported monolayer using a simpler model with d bands only reports $D = 210$ meV Å^2.

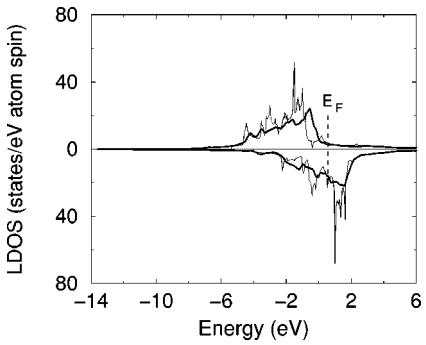

FIG. 3. Local density of states for majority and minority spins calculated for an Fe monolayer adsorbed on W(110) (thick line) and for a free-standing Fe(110) monolayer (thin line). The upper (lower) part of the figure corresponds to majority- (minority-) spin states, and the vertical dashed line marks the position of the Fermi energy.

B. Short-wavelength spin waves

We now investigate the whole spin wave spectrum by calculating $\chi^{+-}(\vec{q}_\parallel,\omega)$ from Eq. (9) as a function of ω for different $\vec{q}_\parallel$. The energy to excite a spin wave with wave vector $\vec{q}_\parallel$ may be obtained from the positions of the peaks in $\mathrm{Im}\,\chi^{+-}(\vec{q}_\parallel,\omega)$, and the corresponding spin-wave lifetimes are inversely proportional to the widths of such peaks.

As we pointed out earlier, the effective Coulomb interaction U appears explicitly in the calculation of $\chi^{+-}(\vec{q}_\parallel,\omega)$. Therefore, we need a prescription for obtaining not only the exchange splittings required for calculating the long-wavelength spin-wave energies, but all Coulomb matrix elements $U_{\mu\nu,\mu'\nu'}$. A reasonable and broadly used approach is to assume a parametrized form of interaction and adjust the parameters so as to reproduce some well-established ground-state properties of the system. The effective interaction must, of course, preserve spin rotational invariance in order to satisfy the Goldstone theorem, i.e., so that $\chi^{+-}(\vec{q}_\parallel,\omega)$ has a pole at $\vec{q}_\parallel=0$. It must also keep the Hamiltonian invariant under the spatial symmetry group operations. We shall experiment with different forms of parametrization of the on-site Coulomb interaction in our calculations of $\chi^{+-}(\vec{q}_\parallel,\omega)$ to test the sensitivity of the results to the various model forms. Before doing so, we notice that for each value of $\vec{q}_\parallel$, the magnetic form factors in Eq. (5) provide basically an overall scaling factor for $\chi^{+-}(\vec{q}_\parallel,\omega)$, which generally decreases with increasing values of $q_\parallel$. Here, for simplicity, we neglect their $\vec{q}_\parallel$ dependence and approximate them by their values at $\vec{q}_\parallel=0$, namely, $F_{\mu\nu}=\delta_{\mu\nu}$. With this approximation Eq. (5) reduces to $\chi^{+-}(ll';\vec{q}_\parallel,\omega)=\Sigma_{\mu,\nu}G_{\mu\mu,\nu\nu}(ll';\vec{q}_\parallel,\omega)$. While this approximation would surely influence predictions of the wave vector dependence of spin-wave excitation strength as observed in neutron scattering, it has no influence in our studies of either the dispersion relation or Landau damping, since these features are controlled only by the denominator which results from inverting Eq. (6).

We start with a rather simple form of parametrization of the Coulomb interaction, which consists in assuming $U_{\mu\nu,\mu'\nu'}=U\delta_{\mu\nu'}\delta_{\nu\mu'}$ for the d orbitals, as Lowde and Windsor did implicitly in their pioneering work on spin dynamics in Ni.[35] This essentially means that a Coulomb interaction U within each orbital is supplemented by ''Hund's rule'' exchange interactions of the same magnitude between different orbitals.[36] With such an assumption, it is not difficult to show that the on-site interaction reduces to $H_{int}=U(n_i-\frac{1}{4}n_i^2-\vec{S}_i\cdot\vec{S}_i)$, where n_i and $\vec{S}_i$ are the total occupation number and spin operators on site i, respectively. This reveals the full rotational invariance obtained in this scheme both in real and spin space. Actually, this form of parametrization is a special case of a slightly more general one proposed later by Parmenter.[37] It is worth noticing that this scheme leads to a rigid exchange splitting of magnitude $\Delta=Um$ (common to all d orbitals) for the one-electron states. Therefore, by taking $U=1$ eV/μ_B we end up with the same exchange splitting and mean-field ground state we have considered earlier in our calculations of the long-wavelength spin-wave energies.

By substituting such a parametrized form of U into Eq. (6) one immediately obtains

$$G_{\mu\nu,\mu'\nu'}(\vec{q}_\parallel,\omega)=G^0_{\mu\nu,\mu'\nu'}(\vec{q}_\parallel,\omega)-U\sum_\gamma{}'\,G^0_{\mu\nu,\gamma\gamma}(\vec{q}_\parallel,\omega)\sum_\alpha{}'\,G_{\alpha\alpha,\mu'\nu'}(\vec{q}_\parallel,\omega), \tag{30}$$

where the prime in the orbital summations means they are restricted to the d orbitals only. This equation may be solved for $G_{\mu\nu,\mu'\nu'}$ without matrix inversion, giving

$$G_{\mu\nu,\mu'\nu'}=G^0_{\mu\nu,\mu'\nu'}-\frac{U\Lambda^0_{\mu\nu}}{1+U\sum_\alpha{}'\,\Lambda^0_{\alpha\alpha}}\sum_\gamma{}'\,G^0_{\gamma\gamma,\mu'\nu'}, \tag{31}$$

where $\Lambda^0_{\mu\nu}=\Sigma'_\gamma G^0_{\mu\nu,\gamma\gamma}$. Owing to the approximation made for form factors and by further assuming the dominant contributions to $\chi^{+-}(\vec{q}_\parallel,\omega)$ come from the d orbitals, we may write

$$\chi^{+-}(\vec{q}_\parallel,\omega)=\frac{\chi^0(\vec{q}_\parallel,\omega)}{1+U\chi^0(\vec{q}_\parallel,\omega)}, \tag{32}$$

where $\chi^0(\vec{q}_\parallel,\omega)=\Sigma'_\mu\Lambda^0_{\mu\mu}=\Sigma'_{\mu\nu}G^0_{\mu\mu,\nu\nu}(\vec{q}_\parallel,\omega)$. The expression in Eq. (32) is formally the same as one obtains for a single-band model, except for the definition of $\chi^0(\vec{q}_\parallel,\omega)$, which contains multiband effects.

Our results for $\mathrm{Im}\,\chi^{+-}(\vec{q}_\parallel,\omega)$ calculated on this basis are shown in Fig. 4. We clearly see that the spin-wave peaks broaden and diminish in height very rapidly with increasing $q_\parallel$, revealing how strongly damped the short-wavelength spin waves become, due to their decay to Stoner excitations. The strength of the spin-wave peaks is expected to fall off more quickly when the $\vec{q}_\parallel$ dependence of the magnetic form factors are taken into account. In Fig. 5 we compare the spin-wave energies extracted from the position of the peaks in $\mathrm{Im}\,\chi^{+-}(\vec{q}_\parallel,\omega)$ with those calculated earlier using the

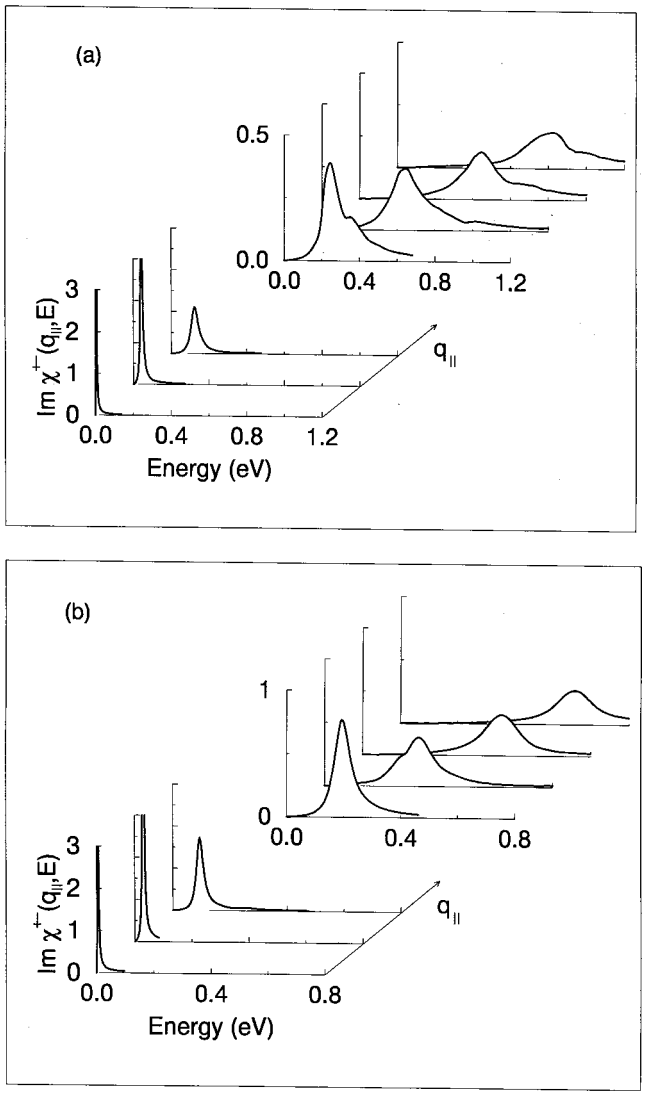

FIG. 4. $\mathrm{Im}\,\chi^{+-}(\vec{q}_{\parallel},E)$ calculated as functions of energy E for different values of the wave vector $\vec{q}_{\parallel}$ along the Γ-X (a) and Γ-L (b) directions of the two-dimensional Brillouin zone for Fe/W(110). The calculations were made within the framework of the Lowde-Windsor treatment of the effective Coulomb interaction (see text). The vertical (y-axis) scale is plotted in arbitrary units. The curves depicted in (a) were calculated for reduced values of $q_{\parallel}=0.05$, 0.15, 0.25, 0.35, 0.45, 0.55, and 0.70, along Γ-X. Those depicted in (b) were calculated for reduced values of $q_{\parallel}=0.10$, 0.20, 0.30, 0.40, 0.50, 0.60, and 0.70, along Γ-L. The numerical integrations were performed with 1036 special points inside the irreducible two-dimensional Brillouin zone.

static approach. For relatively low values of $\vec{q}_{\parallel}$, the results obtained by both approaches are in excellent agreement, as they must be, but they differ substantially for larger values of $\vec{q}_{\parallel}$, as expected. We see very clearly from this figure that dispersion curves generated by adiabatic theory cannot be viewed as quantitative beyond small wave vectors where quadratic behavior obtains.

Within the framework of the Lowde-Windsor treatment of the intra-atomic Coulomb interaction, we found no multi-

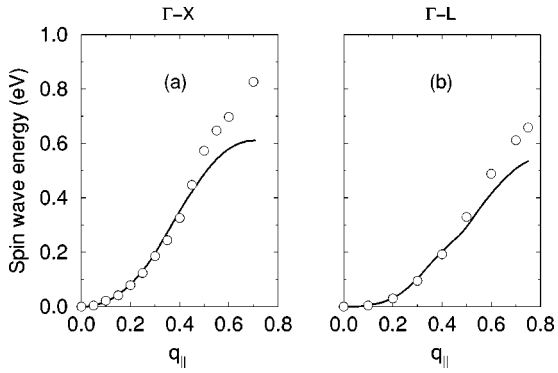

FIG. 5. Spin-wave dispersion relations calculated for Fe/W(110) as functions of $\vec{q}_{\parallel}$ along the Γ-X (a) and Γ-L (b) directions of the two-dimensional Brillouin zone. The open circles were obtained from the maxima positions of the spin-wave spectra given by the dynamical RPA susceptibility, as illustrated in Fig. 4. The solid lines were calculated from the static susceptibility by using Eq. (26) (see text).

peak structures in $\mathrm{Im}\,\chi^{+-}(\vec{q}_{\parallel},\omega)$ which can be interpreted as evidence of "optical-spin-wave" modes or gaps in the dispersion relation with the character of hybridization gaps. We note that the authors of Ref. 7 failed to find such features as well in their studies of spin waves in bulk Fe. Such features were first reported by Cooke *et al.*,[17] who predicted a doublet structure in $\mathrm{Im}\,\chi^{+-}(\vec{q},\omega)$ for wave vectors along [100] in studies of spin waves in bulk Fe. In a later paper, a three-peak structure was reported at some wave vectors also along [100] in bulk Fe.[38] The high-frequency members of such structures were argued to be "optical spin waves." Similar structures have been reported in other theoretical studies as well. For instance, in Ref. 39, for spin waves along the [100] direction of Ni, such structures appear at $q \approx 0.2(2\pi/a_0)$ and extend out to the Brillouin zone boundary. Calculations by Savrasov[40] reveal a doublet along the [100] direction of Ni, but only for a very restricted range of wave vectors, to produce a spin-wave dispersion with an apparent hybridization gap. His calculations, however, show no multipeak structures in the spin-wave spectrum of bulk Fe for wave vectors along the same direction, in sharp contrast with what has been predicted by Refs. 17 and 38. Calculations by Karlson and Aryasetiawan[41] produce a gap for a wave vector along [111] of Ni, while no such feature was reported by Cooke and collaborators[39] or Savrasov.[40] The theoretical literature on "optical spin waves" or apparent hybridization gaps in the spin-wave dispersion relations of bulk Fe and bulk Ni is thus quite confusing, since no two papers produce the same features. We shall show in some cases that these structures are artifacts produced by numerical calculations that have failed to converge and, in one instance, due to the use of an inappropriate form for the intra-atomic Coulomb interaction. We illustrate the former point in Fig. 6, and we comment on the second in the discussion which follows.

In Fig. 6(a), for a reduced wave vector $q_{\parallel}=0.25$ along Γ-X, we show two calculations of $\mathrm{Im}\,\chi^{+-}(\vec{q}_{\parallel},\omega)$ for two choices of the $\vec{k}_{\parallel}$-space integration grid. In one we use 262 special points[42] in the irreducible two-dimensional Brillouin

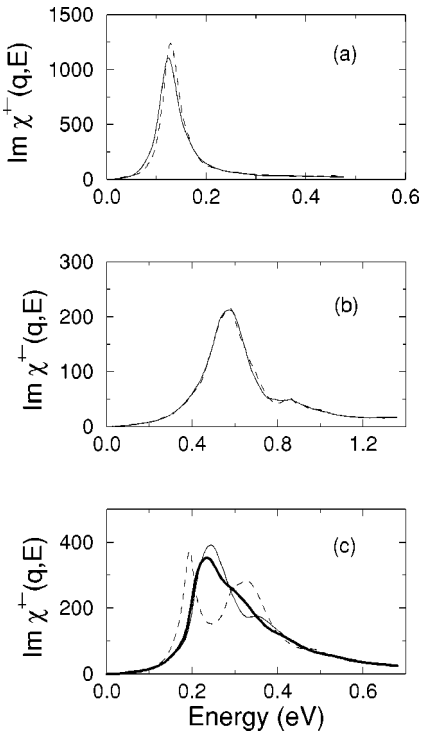

FIG. 6. Comparison between the spin-wave spectra for Fe/W(110) calculated as functions of energy E with different number of points in the $\vec{k}_{\parallel}$-space integration grid for three distinct values of $\vec{q}_{\parallel}$ along the Γ-X direction in the two-dimensional Brillouin zone. (a), (b), and (c) represent results for reduced values of $q_{\parallel}=0.25$, 0.50, and 0.35, respectively. The dashed curves were obtained with 262 special points in the irreducible two-dimensional Brillouin zone and the thin solid curves with 1036 points. The thick solid line depicted in (c) was calculated with 4120 points in the irreducible two-dimensional Brillouin zone. All calculations were made with the effective Coulomb interaction treated according with the Lowde-Windsor parametrization scheme (see text).

zone, and in the second we use 1036 points. The two results are in excellent accord, so the calculation based on the coarse grid has converged nicely. In Fig. 6(b), we show a similar comparison for $q_{\parallel}=0.50$ along the same direction to reach the same conclusion. Now, for $q_{\parallel}=0.35$, the calculation based on the coarse grid produces a very clear doublet in the spectral density, quite similar to those displayed in various earlier papers.[41,17] However, as we increase the number of points in the integration grid, the doublet evolves into a single peak, with at most some asymmetry. In our studies, save for the case of an inappropriate Coulomb interaction described below, the presence of a doublet in the spectral density was just a signature of a calculation which had not converged. A $\vec{k}_{\parallel}$-space grid which provides convergence at some wave vectors may fail at nearby wave vectors in our experience. All of our converged calculations based on a choice of full rotationally invariant Coulomb interaction produce a single dispersion curve, with no ''optical spin wave'' and with no ''hybridization gaps.'' Our experience thus leads us to treat predictions of such structures with some caution.

It is the case, however, that evidence for ''optical spin waves'' appears in a neutron study of spin waves in bulk Ni.[43] In the paper, unfortunately, no data on the shape of the loss spectrum itself has been provided for wave vectors in the regime where optical spin waves appear in the dispersion relation. It is our understanding that a true double-peaked structure was not found; the presence of the ''optical-spin-wave'' mode was inferred from the modest structure in the wing of the principal spin-wave loss feature.[44] A similar high-energy structure reported in Fe (Ref. 45) and suggested as an optical-spin-wave mode is in very poor quantitative agreement with earlier theoretical predictions,[17,38] but is in excellent accord with more recent studies which interpret this very broad feature as a modest structure in the Stoner spectrum.[46] Clearly, further experimental studies of this issue will prove of great interest.

The spin-wave excitation spectrum is directly affected by the electron-electron interaction and the way it is taken into account at large wave vectors. Some important features of the spectrum, such as the disclosure of possible multiple spin-wave modes, for example, may depend upon the form of parametrization used, as well as on the choice of those parameters, especially for relatively large wave vectors along certain directions. In order to investigate the relationship between the effective Coulomb interaction and the spin-wave excitation spectra, we have carried out calculations of $\chi^{+-}(\vec{q},\omega)$ using other parametrized forms of interaction. We turn to these studies next. We shall see that the predictions presented here are robust in regard to the sensitivity to the choice of Coulomb interaction, as long as the choice satisfies constraints imposed by rotational symmetry.

C. Other forms of parametrization for the effective Coulomb interaction

A more comprehensive scheme for parametrizing the electron-electron interaction in ferromagnetic transition metals has been recently proposed.[7,22] It assumes that the effective on-site Coulomb interaction between the $3d$ electrons has full rotational symmetry. This allows all Coulomb matrix elements $U_{\mu\nu,\mu'\nu'}$ between the d orbitals to be expressed in terms of just three independent quantities, which may be treated as adjustable parameters to fit ground-state properties of the system.[7] Such an atomiclike scheme of dealing with the Coulomb interaction is compatible with methods used in atomic physics literature to describe intra-d-shell excitations[23,47] and characterizes the Coulomb interaction structure appropriately in the limit of separated atoms. A detailed study of the spin-wave excitations in an unsupported ultrathin ferromagnetic Fe(100) film and in bulk Fe has been made using this approach.[7] It provides a bulk spin-wave exchange stiffness in excellent accord with previous calculations and with neutron measurements. A very good account of the high-energy spectrum was also obtained, with no evidence of an optical spin-wave branch, however, in agreement with Savrasov's recent calculations for bulk Fe.[40]

We have employed this form of parametrization to calculate the spin-wave spectra in Fe/W(110). In our calculations we have used the Coulomb parameters obtained for bulk Fe that are listed in the second row of Table 2 of Ref. 7. They lead to a mean-field self-consistent ground-state magnetic

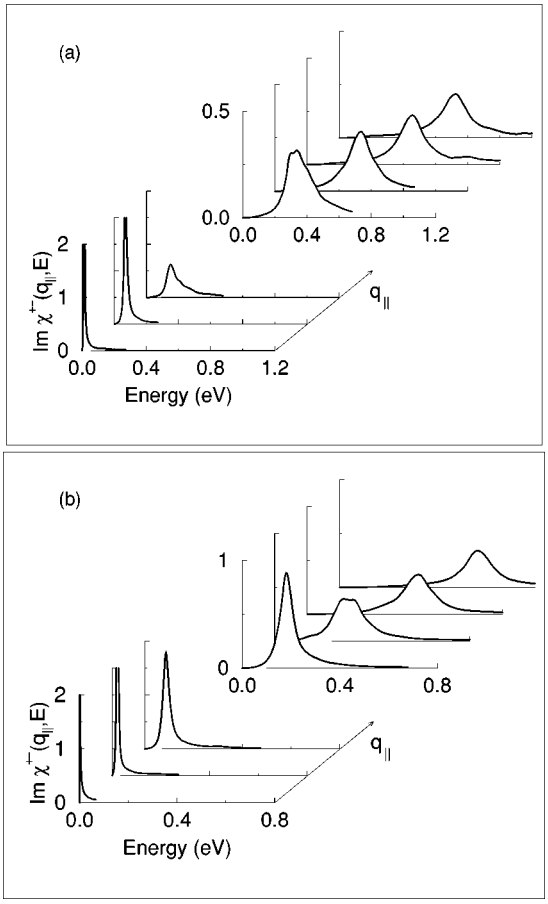

FIG. 7. Im $\chi^{+-}(\vec{q}_\parallel,E)$ calculated for Fe/W(110) as functions of energy E for different values of the wave vector $\vec{q}_\parallel$ along the Γ-X (a) and Γ-L (b) directions of the two-dimensional Brillouin zone. The curves represent results calculated for reduced values of $q_\parallel = 0.10$, 0.20, 0.30, 0.40, 0.50, 0.60, and 0.70. The numerical integrations were performed with 1036 special points in the irreducible two-dimensional Brillouin zone. The vertical (y-axis) scale is plotted in arbitrary units. The results shown here have been obtained by employing the parametrization scheme developed in Ref. 7 for treating the effective Coulomb interaction (see text).

moment $m = 2.18\mu_B$ for the Fe overlayer film. The results for the spin-wave spectra are shown in Fig. 7. They depict basically the same overall qualitative behavior as found in the previous section, namely, a rapid decrease in intensity with concurrent broadening of the spin wave peak as $\vec{q}_\parallel$ increases. We have also found no clear evidence of spin-wave hybridization gaps due to the presence of optical-spin-wave modes with this form of parametrization. We may notice a broad and relatively shallow double-peak structure in the spin-wave spectra for $q_\parallel = 0.4$ along ΓX and for $q_\parallel = 0.5$ along ΓL. Such features, however, disappear when the precision of our Brillouin zone numerical integration is increased, as illustrated in Fig. 8. The corresponding spin-wave energies estimated from the peak positions in the spectra are shown in Fig. 9, where they are compared with those obtained in the previous section. We are reassured by the fact that the quantitative difference between these two schemes are very small.

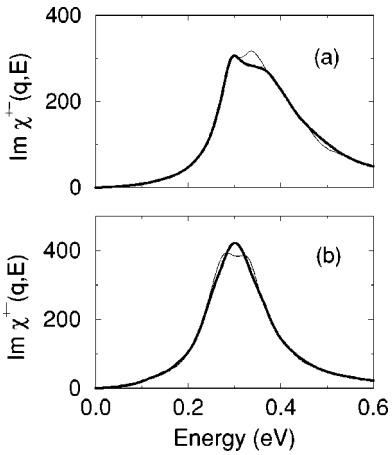

FIG. 8. Im $\chi^{+-}(\vec{q}_\parallel,E)$ calculated for Fe/W(110) with different number of points in the $\vec{k}_\parallel$-space integration grid. Results of Im $\chi^{+-}(\vec{q}_\parallel,E)$ are shown as functions of energy E for reduced values of $q_\parallel = 0.4$ (a) and $q_\parallel = 0.5$ (b) along the Γ-X and Γ-L directions in the two-dimensional Brillouin zone, respectively. The thin lines were calculated with 1036 special points in the irreducible two-dimensional Brillouin zone and the thick lines with 4120 special points. Both calculations were made employing the parametrization scheme developed in Ref. 7 for treating the effective Coulomb interaction (see text).

Apparent hybridization gaps in the dispersion relation of spin waves in itinerant ferromagnets were first predicted by Cooke and collaborators,[17] as noted above. In their original calculations for bulk Fe and Ni, they retained only the diagonal elements of the U matrix, assuming $U_{\mu\nu,\mu'\nu'} = U_\mu \delta_{\nu\mu}\delta_{\mu'\mu}\delta_{\nu'\mu}$, where the $U_\mu \equiv U_{\mu\mu,\mu\mu}$ are equal for all μ belonging to the same irreducible representation of the point symmetry group. With this assumption, the exchange splittings of the electronic states are given by $\Delta_\mu = U_\mu m_\mu$ and the dimensions of the matrices involved in Eq. (9) are considerably reduced, because in this case Eq. (6) includes

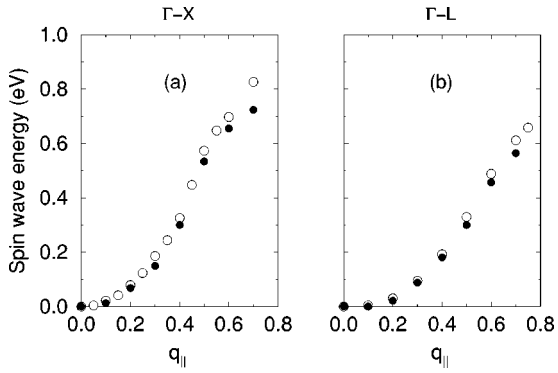

FIG. 9. Comparison between spin-wave dispersion relations calculated for Fe/W(110) using different parametrization schemes to treat the effective Coulomb interaction. Open circles represent results obtained within the framework of the Lowde-Windsor parametrization scheme and solid circles with the parametrization scheme developed in Ref. 7. Calculated values are shown for $\vec{q}_\parallel$ along the Γ-X (a) and Γ-L (b) directions of the two-dimensional Brillouin zone.

only G-matrix elements of the type $G_{\gamma,\eta} \equiv G_{\gamma\gamma,\eta\eta}$ and $G^0_{\gamma,\eta} \equiv G^0_{\gamma\gamma,\eta\eta}$. Cooke and collaborators considered two values of U_μ, corresponding to the t_{2g} and e_g cubic symmetries, and treated $U_{t_{2g}}$ and U_{e_g} as adjustable parameters, which they determined by fitting the observed total magnetic moment and its t_{2g} to e_g character. The corresponding exchange splittings obtained by such a procedure turned out to be essentially identical for bulk Fe. They found spin-wave stiffness constants in good agreement with experiments for both bulk Fe and Ni. However, as pointed out by Edwards[48] and Allan,[36] the assumption of a diagonal U matrix is not compatible with rotational invariance under the full O_h cubic spatial symmetry group, and thus the scheme is quite unphysical in character.

Cooke and Blackman eventually discovered the difficulty with their original parametrization and have used Coulomb potentials with proper rotational symmetry in some of their later papers.[38,22] For completeness, we have also calculated the spin-wave spectra for the Fe monolayer adsorbed on W(001) employing Cooke's original form of Coulomb interaction. Here, the bulk t_{2g} and e_g manifolds split into four different structures due to the reduced symmetry in the adsorbed film. In order to keep the number of parameters to a minimum and to make contact with the long-wavelength calculations performed in Sec. III A, we consider a single exchange splitting $\Delta_\mu = Im$ common to all d orbitals, with $I = 1$ eV/μ_B. This is equivalent to assuming an effective Coulomb interaction $U_\mu = Im/m_\mu$. Our results for $\mathrm{Im}\,\chi^{+-}(\vec{q}_\parallel,\omega)$ calculated for several wave vectors along both the Γ-X and Γ-L directions are shown in Fig. 10. The most striking features are the distinct doublets that appear in the spin-wave spectrum. They are clearly visible in Figs. 10(a) and 10(b) for $q_\parallel = 0.3$ and $q_\parallel = 0.6$ along the Γ-X and Γ-L directions, respectively. Contrary to the previous cases we have discussed above, these doublets are not artifacts of poorly converged $\vec{k}_\parallel$-space numerical integration, but a consequence of this Coulomb interaction parametrization form. The corresponding spin-wave dispersion relations are shown in Fig. 11 in comparison with those we have evaluated previously using other forms of Coulomb interaction. With this inappropriate assumption of a diagonal U matrix, hybridization gaps apparently open up in the spin-wave dispersion relation at reduced values of $q_\parallel = 0.3$ and $q_\parallel = 0.6$ along the Γ-X and Γ-L directions, respectively. The spectra become very broad as $q_\parallel$ increases towards the Brillouin zone boundary and the determination of their maxima somewhat inaccurate, particularly for $\vec{q}_\parallel$ along Γ-X; estimates of such uncertainties are represented by vertical lines in Fig. 11(a). The doublet structures for $\vec{q}_\parallel$ along Γ-L remain reasonably well defined, beyond $q_\parallel = 0.6$, all the way to the Brillouin zone boundary.

It is, therefore, clear that the appearance of hybridization gaps in calculated spin-wave dispersion relations of itinerant ferromagnets also depends upon the manner by which the effective Coulomb interaction is treated. Such dependence becomes even more impressive in the case of a free-standing monolayer, where the assumption of a diagonal U matrix with elements $U_\mu = Im/m_\mu$ yields four distinct spin-wave

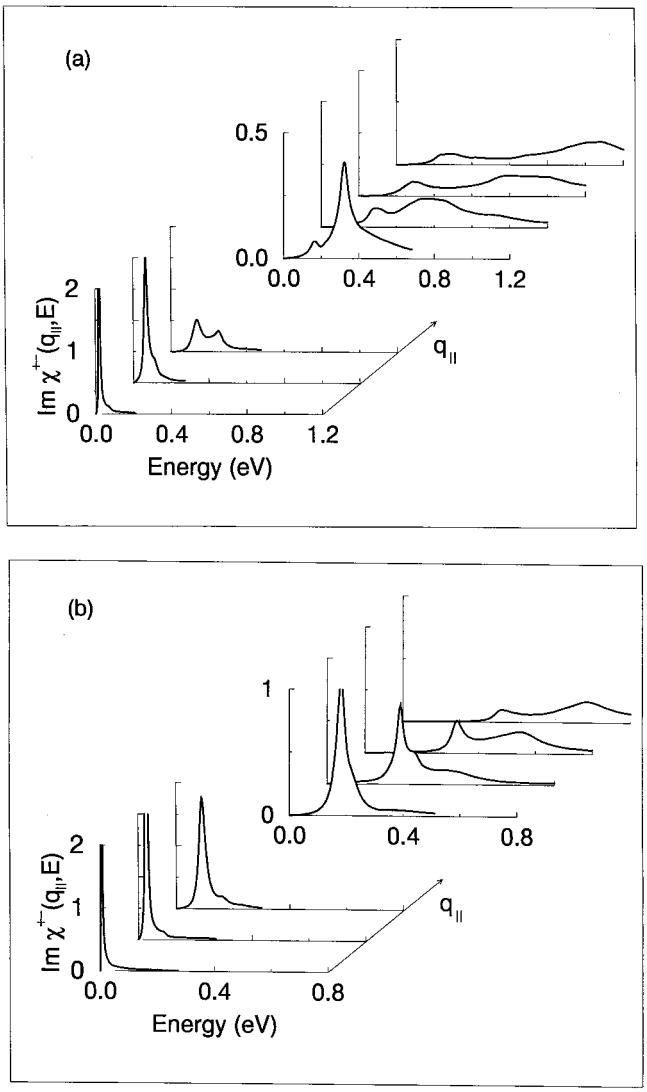

FIG. 10. $\mathrm{Im}\,\chi^{+-}(\vec{q}_\parallel,E)$ calculated for Fe/W(110) as functions of energy E for different values of the wave vector $\vec{q}_\parallel$ along the Γ-X (a) and Γ-L (b) directions of the two-dimensional Brillouin zone. The curves represent results calculated for reduced values of $q_\parallel = 0.10$, 0.20, 0.30, 0.40, 0.50, 0.60, and 0.70. The numerical integrations were performed with 1036 special points in the irreducible two-dimensional Brillouin zone. The vertical (y-axis) scale is plotted in arbitrary units. The results shown here were obtained by assuming a diagonal effective on-site Coulomb interaction, as originally proposed by Cooke *et al.* (Ref. 17) (see text).

peak structures in $\mathrm{Im}\,\chi^{+-}(\vec{q}_\parallel,\omega)$ for values of $\vec{q}_\parallel$ beyond the long-wavelength regime. This is illustrated by the dotted line in Fig. 12, calculated for $q_\parallel = 0.35(2\pi/a_0)$ along Γ-X. The appearance of those quadruplets is compatible with the local magnetic moment being split into four components with distinct d characters. The assumption of a diagonal- and orbital-dependent U matrix may reduce the on-site magnetic coupling between such components and perhaps allow excitations involving these internal degrees of freedom to show up in the spin-wave spectrum. However, the use of a proper full rotationally invariant Coulomb interaction, such

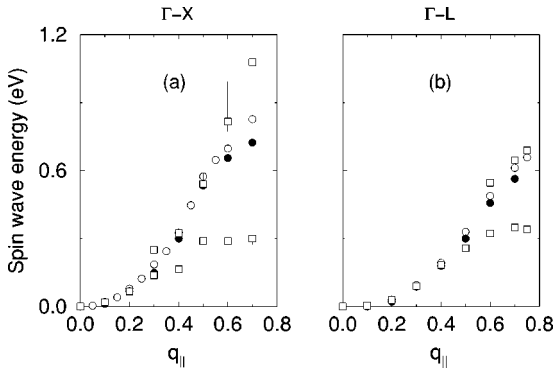

FIG. 11. Comparison between spin-wave dispersion relations calculated for Fe/W(110) using three different parametrization schemes to treat the effective Coulomb interaction. Open circles, solid circles, and open squares represent results obtained with the parametrization schemes employed by Lowde and Windsor, Tang *et al.* (Ref. 7) and that originally considered by Cooke *et al.* (Ref. 17) which assumes a diagonal effective Coulomb U matrix, respectively (see text). The spin-wave dispersions are shown for $\vec{q}_{\parallel}$ along the Γ-X (a) and Γ-L (b) directions of the two-dimensional Brillouin zone. The vertical lines depicted in (a) for some values of $\vec{q}_{\parallel}$ represent estimates of the inaccuracy in determining the maxima of the spectra for the corresponding values of $\vec{q}_{\parallel}$ values.

as the one proposed in Refs. 7 and 22 or that implicitly adopted by Lowde and Windsor, makes those quadruplets disappear and produces a spectrum with only a single spin wave peak structure with no ''optical spin wave'' or ''hybridization gaps,'' as illustrated in Fig. 12. By comparing results depicted in Figs. 12 and 4, we also clearly see that the presence of the tungsten substrate substantially increases the

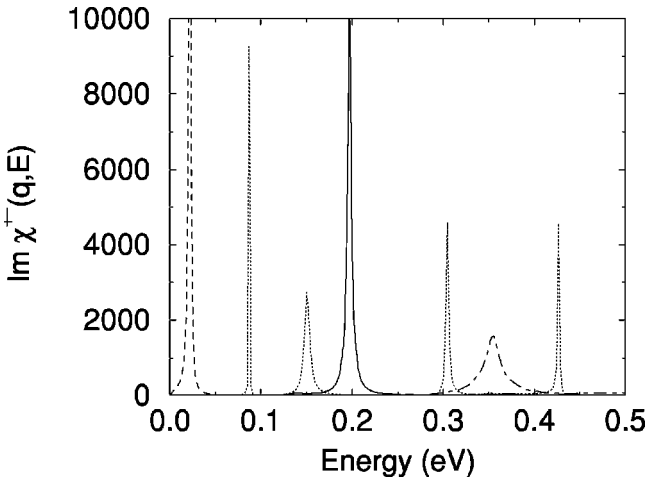

FIG. 12. Im $\chi^{+-}(\vec{q}_{\parallel},E)$ calculated for a free-standing Fe(110) monolayer as functions of energy E for different values of the wave vector $\vec{q}_{\parallel}$ along the Γ-X direction of the two-dimensional Brillouin zone. The dotted curve was calculated for reduced $q_{\parallel}=0.35$ employing Cooke's original parametrization scheme which assumes a diagonal effective on-site Coulomb interaction (see text). The dashed, solid, and dot-dashed lines were calculated within the framework of the Lowde-Windsor parametrization scheme for reduced values of $q_{\parallel}=0.10$, 0.35, and 0.60 along Γ-X, respectively.

spin-wave damping in comparison with the free-standing Fe monolayer. This is in qualitative agreement with results of previous model calculations based on a simple Hubbard Hamiltonian.[31]

IV. SUMMARY AND CONCLUDING REMARKS

In this paper, we have presented an extensive series of theoretical studies of the spin-wave excitations for the ferromagnetic Fe monolayer on W(110). Our empirical tight-binding scheme allows us to carry out model calculations for the case where the W substrate is truly semi-infinite. In our view, this is a most desirable feature of the method since to accurately describe the Landau damping of the short-wavelength spin waves, calculations should be carried out within the framework of a model with a true continuum of Stoner excitation, which serves as final states in the decay process. We do find that the short-wavelength spin waves are quite heavily damped, as we may appreciate from Fig. 4. This feature has its origin in the high density of final states in the W $5d$-band complex. It will be interesting to explore the Landau damping of short-wavelength spin waves as the thickness of the Fe film is increased or if the ultrathin film is adsorbed on a noble-metal substrate. Studies of the first point are underway and of the second point will be undertaken in the near future. One disadvantage of our scheme, when compared with full *ab initio* methods, is that the on site Coulomb interactions are described in an empirical manner with use of adjustable parameters. To explore the sensitivity of our predictions to this aspect of our model, we have carried out calculations with two different schemes, each compatible with the requirement of local site symmetry and spin rotation invariance. The two schemes[7,35] produce results that are very similar indeed from the quantitative point of view, as one may see from Fig. 5.

We have also compared results generated within the framework of an adiabatic description of spin motions to that provided by the full dynamical theory to see that they agree in regard to the value of the exchange stiffness, but the adiabatic approach provides poor quantitative results for short wavelengths. Of course, within the framework of the adiabatic, the strong Landau damping present at short wavelengths is absent from the theory. We remind the reader again of the discussion presented some years ago by Edwards and Muniz,[18] who proved that the adiabatic approach only provides reliable results at long wavelengths, where the spin-wave excitation energy varies quadratically with wave vector. We have extended their proof to the case of an adsorbed ferromagnetic film for a general form of Coulomb interaction, and an expression for the exchange stiffness in this case may be extracted from Eq. (26), evaluated for small $\vec{q}_{\parallel}$.

We find that for the ferromagnetic the monolayer, the spin-wave dispersion relation is highly anisotropic with spin waves in the Γ-X direction substantially stiffer than those in the Γ-L direction. Our calculated exchange stiffness along Γ-X is $D_{\Gamma X}=400$ meV Å^2, while along Γ-L we have $D_{\Gamma L}=107$ meV Å^2. The anisotropy in the exchange stiffness is much larger for the adsorbed monolayer than for a free-standing monolayer. We note that a simple nearest-neighbor

Heisenberg model would lead to a value of D along Γ-X twice as large as that along Γ-L. Interestingly, as $q_\parallel$ increases, our dispersion relation along Γ-L rises above the extrapolation of the quadratic form $Dq_\parallel^2$. As the Fe thickness is increased, the anisotropy in the exchange stiffness must decrease, since in bulk Fe symmetry requires the dispersion relation to be isotropic in the long-wavelength limit. This question is under study currently.

We have also explored the question of whether ''optical spin waves'' exist or whether hybridization gaps might be present in the dispersion relation of spin waves in the Fe monolayer. At least for our preferred methods of representing the Coulomb interaction,[7,35] we have found no clear evidence of ''optical spin waves'' in the spin-wave excitation spectra. Under certain circumstances, we find structures in the spectral density, very similar to those usually associated with hybridization gaps, but in our experience they are a consequence of poorly converged calculations. A tricky issue, as illustrated in Fig. 6, is that one may achieve numerical convergence at most wave vectors in the Brillouin zone, but at selected points where anomalous features are found, particular care must be exercised to ensure convergence has been achieved.

It is our hope that calculations such as those presented here will stimulate new experimental studies of spin-wave excitations in ultrathin films via the SPEELS technique, which in our view should allow experimental access to the issues explored in the present paper.

ACKNOWLEDGMENTS

R.B.M. has benefited greatly from conversations with A.T. Costa, Jr., M. Plihal, and D.M. Edwards. This work has been supported by the U.S. Department of Energy, through Grant No. DE-FG03-84ER 45083. R.B.M. also acknowledges partial financial support by CNPq (Brazil).

*Permanent address: Instituto de Física, Universidade Federal Fluminense, 24210-340 Niterói, RJ, Brazil.

[1] For a review, see A.J. Freeman and R.Q. Wu, J. Magn. Magn. Mater. **100**, 497 (1991).

[2] B. Heinrich, in *Ultrathin Magnetic Structures*, edited by B. Heinrich and J.A.C. Bland (Springer-Verlag, Heidelberg, 1994), Vol. 2, p. 195.

[3] J.F. Cochran, in *Ultrathin Magnetic Structures* (Ref. 2), p. 222.

[4] While the exchange stiffness enters the description of the modes excited in such experiments, this is in fact a material property that may be deduced from a study of the ground-state energy of a ferromagnet placed in a static magnetic field which exhibits a long-wavelength spatial variation.

[5] For examples of such studies and related theoretical analysis, see Burl M. Hall, D.L. Mills, M.H. Mohamed, and L.L. Kesmodel, Phys. Rev. B **38**, 5856 (1988); S. Lehwald, F. Wolf, H. Ibach, Burl M. Hall, and D.L. Mills, Surf. Sci. **192**, 131 (1987).

[6] M.P. Gokhale, A. Ormeci, and D.L. Mills, Phys. Rev. B **46**, 8978 (1992).

[7] H. Tang, M. Plihal, and D.L. Mills, J. Magn. Magn. Mater. **187**, 23 (1998).

[8] M. Plihal and D.L. Mills, Phys. Rev. B **52**, 12 813 (1995).

[9] Jisang Hong and D.L. Mills, Phys. Rev. B **61**, R858 (2000).

[10] M. Plihal, D.L. Mills, and J. Kirschner, Phys. Rev. Lett. **82**, 2579 (1999).

[11] J. Kirschner (private communication).

[12] See the discussion in U. Gradmann, J. Magn. Magn. Mater. **100**, 481 (1991).

[13] C.S. Wang, R.E. Prange, and V. Korenman, Phys. Rev. B **25**, 5766 (1982).

[14] M. Pajda, J. Kudrnovský, I. Turek, V. Drchal, and P. Bruno, Phys. Rev. Lett. **85**, 5424 (2000); Phys. Rev. B **64**, 174402 (2001).

[15] M.I. Katsnelson and A.I. Lichtenstein, Phys. Rev. B **61**, 8906 (2000).

[16] S.V. Halilov, A.Y. Perlov, P.M. Oppeneer, and H. Eschrig, Europhys. Lett. **39**, 91 (1997).

[17] J.F. Cooke, J.W. Lynn, and H.L. Davis, Phys. Rev. B **21**, 4118 (1980); see also Ref. 38.

[18] D.M. Edwards and R.B. Muniz, J. Phys. F: Met. Phys. **15**, 2339 (1985).

[19] R.P. Erickson and D.L. Mills, Phys. Rev. B **43**, 1187 (1991).

[20] J.C. Slater and G.F. Koster, Phys. Rev. **94**, 1498 (1954).

[21] A. Umerski, Phys. Rev. B **55**, 5266 (1997); M.P.L. Sancho, J.M.L. Sancho, and J. Rubio, J. Phys. F: Met. Phys. **15**, 851 (1985).

[22] J.M. Bass, J.A. Blackman, and J.F. Cooke, Phys. Rev. B **53**, 2556 (1996).

[23] M. Tinkham, *Group Theory and Quantum Mechanics* (McGraw-Hill, New York, 1964).

[24] S. Frota-Pessôa, R.B. Muniz, and J. Kudrnovský, Phys. Rev. B **62**, 5293 (2000).

[25] M.V. Tovar Costa, A.C. de Castro Barbosa, R.B. Muniz, and J. d'Albuquerque e Castro, Phys. Rev. B **65**, 052401 (2001).

[26] S.B. Legoas, A.A. Araujo, B. Laks, A.B. Klautau, and S. Frota-Pessoa, Phys. Rev. B **61**, 10 417 (2000); we kindly thank S.F. Pessôa for providing the tight-binding parameters for bulk W.

[27] R.H. Victora, in *Magnetic and Electronic Properties of Low-dimensional Systems*, edited by L.M. Falicov and J.L. Moran-Lopez (Springer, Berlin, 1986), p. 25.

[28] S.C. Hong and A.J. Freeman, and C.L. Fu, Phys. Rev. B **38**, 12 156 (1988).

[29] O. Gunnarson, J. Phys. F: Met. Phys. **6**, 587 (1976).

[30] F.J. Himpsel, Phys. Rev. Lett. **67**, 2363 (1991).

[31] L.H.M. Barbosa, R.B. Muniz, A.T. Costa, and J. Mathon, Phys. Rev. B **63**, 174401 (2001).

[32] J. Rath and A.J. Freeman, Phys. Rev. B **11**, 2109 (1975).

[33] R. Wu (private communication).

[34] J. d'Albuquerque e Castro, D.M. Edwards, J. Mathon, and R.B. Muniz, J. Magn. Magn. Mater. **93**, 295 (1991).

[35] R.D. Lowde and C.G. Windsor, Adv. Phys. **19**, 813 (1970).

[36] D.M. Edwards, in *Moment Formation in Solids*, edited by W.J.L. Buyers, Vol. 117 of *NATO Advanced Study Institute, Series B: Physics* (Plenum, New York, 1984), p. 114.

[37] R.H. Parmenter, Phys. Rev. B **8**, 1273 (1973).

[38] J.A. Blackman, T. Morgan, and J.F. Cooke, Phys. Rev. Lett. **55**, 2814 (1985).

[39] J.F. Cooke, J.A. Blackman, and T. Morgan, Phys. Rev. Lett. **54**, 718 (1985).
[40] S.Y. Savrasov, Phys. Rev. Lett. **81**, 2570 (1998).
[41] K. Karlsson and F. Aryasetiawan, Phys. Rev. B **62**, 3006 (2000); J. Phys.: Condens. Matter **12**, 7617 (2000).
[42] S.L. Cunningham, Phys. Rev. B **10**, 4988 (1974).
[43] H.A. Mook and D. McK. Paul, Phys. Rev. Lett. **54**, 227 (1985).
[44] H.A. Mook (private communication).
[45] A.T. Boothroyd, T.G. Perring, A.D. Taylor, D. McK. Paul, and H. Mook, J. Magn. Magn. Mater. **104-107**, 713 (1992); T.G. Perring, A.T. Boothroy, D.McK. Paul, A.D. Taylor, R. Osborn, R.J. Newport, J.A. Blackman, and H.A. Mook, J. Appl. Phys. **69**, 6219 (1991).
[46] See Fig. 5 of Ref. 7 and associated discussion.
[47] J.S. Griffith, *The Theory of Transition-Metal Ions* (Cambridge, University Press, Cambridge, England, 1961).
[48] S.R. Allan, Ph.D. thesis, Imperial College, London, 1982.